Laboratory and Synchrotron Radiation total – reflection X-ray fluorescence: New Perspectives in Detection Limits and Data Analysis

K. Baur [1*], S. Brennan [1], B. Burrow [2] , D. Werho [3] and P. Pianetta [1]

1 Stanford Synchrotron Radiation Laboratory, Stanford CA. E-mail: baur@slac.stanford.edu

2 ACCUREL. 350 Potrero Avenue, Sunnyvale CA

3 Motorola, Inc., Mesa AZ

Having established detection limits for transition elements exceeding current requirements of the semiconductor industry, our recent efforts at the Stanford Synchrotron Radiation Laboratory (SSRL) have focused on the improvement of the detection sensitivity for light elements such as Al. Data analysis is particularly challenging for Al, due to the presence of the neighboring Si signal from the substrate. Detection limits can be significantly improved by tuning the excitation energy below the Si-K absorption edge. For conventional TXRF systems this can be done by using a W-Mα fluorescence line (1.78 keV) for excitation. At a synchrotron radiation facility energy tunability is available. However, in both cases this results in a substantial increase in background due to resonant x-ray Raman scattering. This scattering dominates the background under the Al Kα fluorescence line, and consequently limits the achievable sensitivity for the detection of Al surface contaminants. In particular, we find that for a precise determination of the achievable sensitivity, the specific shape of the continuous Raman background must be taken into account in the data analysis. The data deconvolution presented here opens a new perspective for conventional TXRF systems to mitigate this background limitation. This results in a minimum detection limit of 2.4 x 10^9 atoms /cm^2 for Al.

Based on these results it will also be demonstrated that by improving the detector resolution, the minimum detection limit can be improved significantly. For a detector resolution of 15 eV as predicted for novel superconducting tunnel junction detectors, an improvement in minimum detection limit of about a factor of 3 can be estimated.

Keywords: Total reflection X-ray fluorescence, low Z elements, Stanford Synchrotron Radiation Laboratory

Introduction

Exploiting the unique capabilities of synchrotron radiation, total reflection x-ray fluorescence spectroscopy (TXRF) has been successfully applied to detect very low concentrations of impurities on Si wafer surfaces [1, 2, 3, 4]. Synchrotron radiation offers several advantages over conventional x-ray tubes: It provides a high incident flux, especially from insertion devices, it is both low-divergence and linearly polarized, which leads to an increased fluorescence signal while reducing the elastically scattered background. In addition, tuning the x-ray energy to a characteristic absorption threshold of a typical element present in the wafer surface increases the excitation cross-section for this element which leads to higher fluorescence intensities. With these combined capabilities we routinely achieve an minimum detection limit of $< 9 \times 10^7$ atoms/cm^2 for transition metals on Si wafer surfaces for a 1000 second spectrum.

On the other hand, the detection of low Z elements such as Al is challenging because of the lower fluorescence yield as compared to transition metals. In addition, the detection of Al on Si wafers is difficult because of the presence of the much stronger Si substrate signal which tends to dominate the spectrum and can easily saturate the semiconductor detector.

However, the latter can be overcome by tuning the primary x-ray energy to an excitation energy below the Si K absorption threshold which also increases the photo absorption cross-section for Al [5, 6]. This results in a minimum detection limit of 2.4 x 10^9 atoms/cm^2 as will be shown below.

For laboratory instruments an acceptable sensitivity for Al detection can be realized by using the W-Mα fluorescence line for primary excitation [7, 8] and attempts have been made by using Si-Kα fluorescence from a Si anode X-ray tube [9]. The x-ray energy of the W-Mα fluorescence line (1.78 keV) is sufficiently below the Si K absorption threshold (1.84 keV) to reduce the substrate signal. A minimum detection limit of about 5 x 10^{10} atoms/cm^2 has been reported for Al.

In both cases, however, one observes a substantial increase in background starting at about 100 eV below the primary excitation energy and extending to lower energies by several hundred eV. This background is due to resonant inelastic x-ray Raman scattering which is an inelastic x-ray scattering process [10, 11, 12]. It has been shown that the asymmetric shape of the x-ray Raman scattering dominates the background of the Al fluorescence line. In order to accurately determine the minimum detection limit, the spectra have to be deconvoluted taking the specific shape of the resonant Raman scattering profile into account [6].

In this paper we demonstrate that this data analysis can also be extended for the deconvolution of TXRF spectra from conventional systems which so far only subtract the background as measured from a clean Si wafer. A deconvolution of the Al spectra would make this step unnecessary and could increase the accuracy in determining the Al concentration on Si wafer surfaces. In addition, based on these results spectra have been

simulated assuming a higher detector energy resolution and the resulting improvement in the minimum detection limit for Al will be discussed.

Experiment

The synchrotron radiation experiments reported here for transition metals were carried out on beam line 6-2 which uses a high flux, 54 pole wiggler on the SPEAR storage ring of the Stanford Synchrotron Radiation Laboratory (SSRL). The tuning range of the double multilayer monochromator which consists of alternating layers of Mo and B_4C (d = 2.9 nm) is set to be between 6 keV and 14 keV. The standard excitation energy for the transition metal analysis is around 11.2 keV which gives a high excitation cross-section for the transition elements such as Fe, Ni and Zn while preventing overlap of the detector escape peak with the fluorescence signals of these elements.

The investigation of low Z elements has been performed at the Jumbo beamline (BL 3-3) at SSRL allowing a softer excitation energy of 1730 eV in order to eliminate the strong Si Kα fluorescence line while simultaneously increasing the absorption cross-section for Al. The beam lines and the general experimental setup used for both the transition metal and light element experiments have been discussed elsewhere [1,6]. The laboratory measurements were performed at Accurel Systems International using a TXRF 300 instrument from Rigaku.

For the transition metal work a wafer from Motorola with very low levels of unintentional Ni and Fe contamination resulting from a state of the art cleaning process has been studied.

The Al spectra have been obtained from standard wafers from Hewlett-Packard Co. with an intentional Al contamination of 8 x 10^{12} atoms/cm^2 for measurements with the conventional Rigaku system and 3 x 10^{11} atoms/cm^2 for the synchrotron radiation based experiments. Both spin-coated wafers have been cross-calibrated in concentration by using inductively coupled plasma mass spectrometry (ICP-MS).

Results and Discussion

Fig. 1 shows the fluorescence spectrum of the Si wafer from Motorola obtained on BL 6-2 after an extended integration time of 5000 seconds. The primary excitation energy has been tuned to be 11280 eV in order to effectively excite transition metals such as Fe and Ni. The spectrum was measured for an angle of incidence of 0.09^o, which is below the critical angle for total external reflection (0.16^o for 11280 eV). The dominant peak at 11280 eV is due to elastic scattering of the primary synchrotron radiation. Next to it one finds its associated escape peak at 9540 eV. The intensity of the Si Kα fluorescence line at 1740 eV has been reduced by a Teflon filter mounted in front of the Si/Li detector in order to reduce the overall count rate load [1]. At 6.4 keV and 7.48 keV the spectrum shows the signatures of the Fe Kα and Ni Kα fluorescence lines from an unintentional surface contamination. Quantification is achieved by comparing the measured peak intensities to the ones of a standard wafer having an intentional contamination of 1 x 10^{11} atoms/cm^2 of Fe, Ni and

Zn. This results in a concentration of 2.5 x 10^8 atoms/cm^2 for Fe and 1.2 x 10^8 atoms/cm^2 for Ni. The background below approximately 7 keV is dominated by the photoelectron bremsstrahlung emitted by the Si 1s photoelectrons which are created in the wafer by the primary photon beam [13]. In the higher energy region the background results from inelastic Compton scattering as well as from the escape peak. The minimum detection limit for Ni is 4.0 x 10^7 atoms/cm^2 for an extended counting time of 5000 seconds corresponding to 8.9 x 10^7 atoms/cm^2 for the standard counting time of 1000 seconds. For Fe the minimum detection limit is higher because the photo absorption cross-section for the chosen primary excitation energy of 11280 eV is reduced by a factor of 0.8 as compared to Ni and because of a higher background contribution in this energy region. The minimum detection limit for Fe is 7.4 x 10^7 atoms/cm^2 for a 5000 second counting time, which corresponds to 1.6 x 10^8 atoms/cm^2 for 1000 seconds. According to its definition [14], the minimum detection limit could be further improved by increasing the incoming photon flux, e.g. by using a third generation synchrotron radiation source such as SPEAR3. This new storage ring at SSRL will be completed in 2003 and will offer several advantages for TXRF. The horizontal source size for an insertion device, which is the dimension of interest given the horizontal reflection geometry being used at SSRL, will be reduced by a factor of 4.65 and the ring current will be increased by a factor of 5. This should result in an overall increase in flux density by about a factor of 23 and should thus improve the minimum detection limit by a factor of 4.8 resulting in a minimum detection limit of about 2 x 10^7 atoms/cm^2 for Ni after a standard 1000 second counting time.

Fig. 2 shows a fluorescence spectrum (dots) obtained on BL 3-3 at SSRL from a wafer intentionally contaminated with 3 x 10^{11} atoms/cm^2 of Al. The spectrum has been taken with an excitation energy of 1730 eV and an angle of incidence of 0.1^o for a 10 000 second count time. The low energy peak is the Al Kα fluorescence signal at 1487 eV and the high energy signal results from the elastically scattered primary photons.

In order to determine the MDL the spectrum has been deconvolved in the energy range between 1000 eV and 2000 eV. The line shape of the Al fluorescence line and the elastically scattered synchrotron radiation is dominated by the detector resolution, which is a Gaussian function with a given full width at half maximum (FWHM) of 100 eV in this energy region. The line shape of the resonant x-ray Raman scattering contribution is determined by the differential cross section for resonant x-ray Raman scattering [15, 16]. Note that the resonant Raman cross-section is convoluted with the detector broadening and that the transmission function of the 5 μm Be window in front of the Si/Li detector is also taken into account. Further details concerning the data analysis and interpretation of the spectra are reported in Ref. [6]. The result, i.e., the sum of the two fitted Gaussian functions and the Raman background, is indicated in Fig. 2 as a solid line. The MDL under these conditions is 6.0 x 10^9 atoms/cm^2 which corresponds to 1.9 x 10^{10} atoms/cm^2 for a standard 1000 s count time. It has been discussed in [6] that this result can be further improved by up to a factor of 8 by increasing the angle of incidence closer to the critical angle (0.9^o at 1730 eV). This should give a minimum detection limit of 2.4 x 10^9 atoms/cm^2 for a 1000 s count time.

Fig. 3 shows the fluorescence spectrum (dots) obtained from a wafer with an intentional Al contamination of 8 x 10^{12} atoms/cm^2 using a TXRF 300 system from Rigaku. This

spectrum has been integrated for 3600 s under an angle of incidence of 0.45^{o} which corresponds to the standard condition for Al detection. In the low energy part one finds the fluorescence signature of the Al Kα line. The dominating contribution in the spectrum at 1.78 keV results from the elastic scattering of the W-Mα excitation line. By comparing the elastic scattering contributions in Fig. 2 and Fig. 3 the advantage of using a linearly polarized excitation source with low divergence such as synchrotron radiation to reduce the amount of elastic scattering becomes clear. The laboratory spectrum has also been deconvolved by using two Gaussian functions representing the Al fluorescence line and the elastically scattered primary radiation having both a fixed FWHM of 130 eV corresponding to the energy resolution at these energies of the Si(Li) detector. The resonant Raman scattering contribution has been determined by convolution of the Raman cross section as calculated for an excitation energy of 1780 eV with the detector broadening (130 eV) multiplied by the transmission function of the 8 μm thick Be window in front of the detector.

The theoretical inelastic resonant Raman scattering profile has been verified by analyzing the spectrum of a clean Si wafer measured under the same experimental conditions with the same Rigaku instrument. The spectrum (dots) is shown in Fig. 4 and shows directly the shape of the low energy tail of the resonant Raman scattering which determines the background under the Al fluorescence line. The inelastic resonant Raman scattering contribution as well as the total fit are also indicated in Fig. 4 as solid lines. Both figures demonstrate that the theoretical modeling curve for the Raman background agrees very well with the experimentally observed background behavior resulting in a minimum detection limit for Al of 4.7×10^{10} atoms/cm^2 for a standard 1000 s count time. This

method can be seen as an alternative to estimating experimentally the background from a clean Si wafer for subsequent background subtraction which is generally less accurate.

To study the influence of energy resolution on the minimum detection limit the spectra shown in Fig.2 and Fig.3 have been simulated for an assumed higher detector energy resolution while maintaining the corresponding solid angles of acceptance. According to the definition of the minimum detection limit [14] this is expected to improve with the square root of the increase in energy resolution.

Higher energy resolution can be achieved experimentally by replacing the Si/Li detector by a wavelength dispersive spectrometer which uses Bragg diffraction from single crystals or multilayers in order to spatially disperse different fluorescence lines corresponding to different wavelengths from each other. Wavelength dispersive spectrometers can easily achieve an energy resolution in the order of a few eV. There are also novel energy dispersive detectors such as superconducting tunnel junctions [17] which have a promising potential for fluorescence spectroscopy as they offer a high energy resolution of around 15 eV at 6 keV photon energy [18]. Also these detectors can be operated at significantly higher count rates than a Si/Li detector, which saturates around 15 000 Hz. The only drawback of these detectors is the relatively small detector area of around (100x100)μm^2 resulting in a much smaller solid angle as compared to a Si/Li detector.

Fig.5 shows the spectrum which would be expected from the Rigaku instrument assuming an energy resolution of 15 eV. It has been simulated by using the intensities of the Al fluorescence line and the elastic scattering contribution as determined from the deconvolution shown in Fig. 3. The intensities of the inelastic Raman scattering

contribution as determined from Fig. 3 have been convoluted with the assumed detector energy resolution of 15 eV. This results in an improved minimum detection limit of 1.4 x 10^{10} atoms/cm^2 for a standard 1000 s count time which is about a factor of 3 better than what can currently be achieved with the Si/Li detector having an energy resolution of 130 eV.

Fig.6 shows the influence of energy resolution improvement on the spectrum which has been taken with synchrotron radiation as primary excitation source. The calculation has been done as discussed for the laboratory case. The increase in energy resolution from 100 eV to 15 eV would improve the minimum detection limit by about a factor of 3 resulting in 6.7 x 10^9 atoms/cm^2 for a 1000 s count time at an angle of incidence of 0.1^o. For an angle of incidence closer to the critical angle for total external reflection the higher detector resolution would even lead to a minimum detection limit of 8.5 x 10^8 atoms/cm^2 for a 1000 s count time

Conclusion

We have demonstrated that the current TXRF setup at SSRL is capable of achieving minimum detection limits for transition metals below 1 x 10^8 atoms/cm^2 for a standard 1000 second integration time. In addition it has been shown that this sensitivity can be further improved by using a third generation synchrotron radiation source which provides a higher flux density.

For the detection of low Z elements on the other hand, the tunability of the synchrotron radiation to lower excitation energies has to be employed in order to reduce the strong Si Kα fluorescence signal. This also increases the photo absorption cross-section for low Z elements. However, this results in an increase in background due to resonant inelastic x-ray Raman scattering. We have developed a method to deconvolute the spectra in order to precisely determine the minimum detection limit. It has been demonstrated that this data analysis can also be applied to spectra obtained from laboratory TXRF instruments using a W-Mα characteristic line for primary excitation. In addition, it has been shown that the minimum detection limit can not only be further improved by increasing the incident flux density as discussed for the case of transition metals but also by increasing the energy resolution of the fluorescence detector. The applicability of such novel detector systems has to be preceded by further detector development including multielement detector arrays to maintain a comparable solid angle to the Si/Li detector.

Figure captions

Fig.1. TXRF spectrum of a Si wafer unintentionally contaminated with Fe and Ni measured for a 5000 second counting time. The spectrum has been taken for a primary x-ray energy of 11280 eV at an angle of incidence of 0.09^{o}.

Fig.2 TXRF spectrum of a wafer intentionally contaminated with Al at a concentration of 3×10^{11} atoms/cm^2 (dots) measured with an excitation energy of 1730 eV on BL 3-3 at SSRL. In addition, the modeled profile of the resonant x-ray Raman scattering including detector broadening is shown (—), as well as the Gaussian fits for the Al signal and the elastic scattering (- - -). The sum of the Gaussian fit and the Raman profile is shown as a solid line.

Fig.3 TXRF spectrum of a wafer intentionally contaminated with Al at a concentration of 8×10^{12} atoms/cm^2 (dots) measured with a laboratory TXRF 300 instrument from Rigaku**.** The modeled profile of the resonant x-ray Raman scattering including detector broadening is included (—), as well as the Gaussian fits for the Al signal and the elastic scattering (- - -). The sum of the Gaussian fit and the Raman profile is shown as a solid line.

Fig.4 TXRF spectrum of a clean Si wafer measured with a laboratory TXRF 300 instrument from Rigaku. The modeled profile of the resonant x-ray Raman scattering contribution including detector broadening as well as the elastic scattering and the total fit are also shown.

Fig.5 Simulation of the spectrum that would results from a laboratory TXRF 300 instrument from Rigaku if the detector energy resolution were of 15 eV**.** The wafer was intentionally contaminated with Al at a concentration of 8×10^{12} atoms/cm^2.

Fig.6 Simulation of a TXRF spectrum measured on BL 3-3 at SSRL with an excitation energy of 1730 eV for an angle of incidence of 0.1^o if the detector resolution were of 15 eV. The wafer was intentionally contaminated with Al at a concentration of 3×10^{11} atoms/cm^2.

Acknowledgements

We would like to thank the staff of SSRL for their expert technical assistance and especially A. Fischer-Colbrie of Hewlett-Packard Co. for providing the Al standards. This work was performed at SSRL, which is supported by the Department of Energy, Office of Basic Energy Science.

References

[1] P. Pianetta, K. Baur, A. Singh, S. Brennan, J. Kerner, D. Werho, J. Wang, Thin Solid Films **373** (2000) 222.

[2] P. Pianetta, N. Takaura, S. Brennan, W. Tompkins, S. S. Laderman, A. Fischer-Colbrie, A. Shimazaki, K. Miyazaki, M. Madden, D. C. Wherry, J. B. Kortright, Rev. Sci. Instrum. **66** (1995) 1293.

[3] F. Comin, M. Navizet, P. Mangiagalli, G. Apostolo, Nucl. Instrum. Meth. **B 150** (1999) 538.

[4] S. Brennan, P. Pianetta, S. Gosh, N. Takaura, C. Wiemer, A. Fischer-Colbrie, S. Laderman, A. Shimazaki, A. Waldhauer, M. A. Zaitz, in Application of Synchrotron Radiation Techniques to Materials Science IV **542**, ed. S. M. Mini, D. L. Perry, S.R. Stock, L. J. Terminello, MRS, Boston (1998).

[5] C. Streli, P. Kregsamer, P. Wobrauschek, H. Gatterbauer, P. Pianetta, S. Pahlke, L. Fabry, L. Palmetshofer, M. Schmeling, Spectrochim. Acta **B54** (1999) 1433.

[6] K. Baur, J. Kerner, S. Brennan, A. Singh, P. Pianetta, J. of Appl. Phys. **88** (2000) 4642.

[7] United States Patent 5732120, March 1998.

[8] T. Fukuda, T. Shoji, M. Funabashi, T. Utaka, T. Arai, K. Miyazaki, A. Shimazaki, R. Wilson, Advances in X-Ray Analysis **39** (1997) 781.

[9] C. Streli et al., Spectrochimica Acta **52B** (1997) 861.

[10] C. J. Sparks, Phys. Rev. Lett. **33** (1974) 262.

[11] F. Gel'mukhanov, H. Agren, Phys. Rep. **312** (1999) 87.

[12] P. Eisenberger, P. M. Platzman, H. Winick, Phys. Rev. Lett. **36** (1976) 623.

[13] N. Takaura, S. Brennan, P. Pianetta, S. Laderman, A. Fischer-Colbrie, J. B. Kortright, D. C. Wherry, K. Miyazaki, A. Shimazaki, Advances in X-Ray Chemical Analysis, Japan **26s** (1995), 113.

[14] E. P. Bertin, Principles and Practice of X-Ray Spectrometric Analysis, New York, Plenum Press (1975).

[15] M. Gavrila, M. N. Tugulea, Rev. Roum. Phys. **20** (1975) 209.

[16] M. Gavrila, Rev. Roum. Phys. **19** (1974) 473.

[17] P. Verhoeve, N. Rando, J. Verveer, A. Peacock, A. van Dordrecht, P. Videler, M. Bavdaz, D. J. Goldie, T. Lederer, F. Scholze, G. Ulm, R. Venn, Phys. Rev. **B53** (1996) 809.

[18] S. Friedrich, M. F. Cunningham, M. Frank, S. E. Labov, A. T. Barfknecht, S. P. Cramer, Nucl. Instr. and Meth. **A444** (2000) 151.

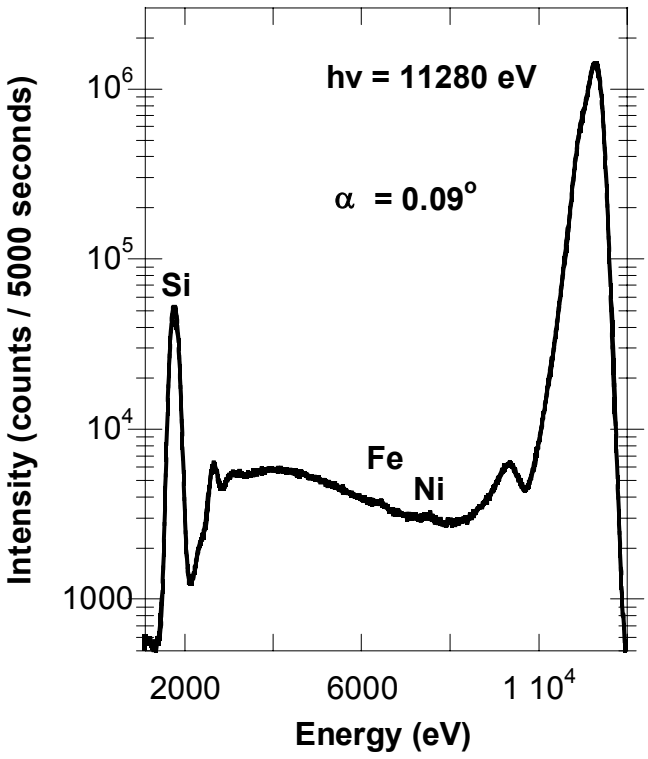
hv = 11280 eV
α = 0.09°
Si
Fe
Ni
Intensity (counts / 5000 seconds)
Energy (eV)
10^6
10^5
10^4
1000
2000
6000
1 10^4

Fig. 1

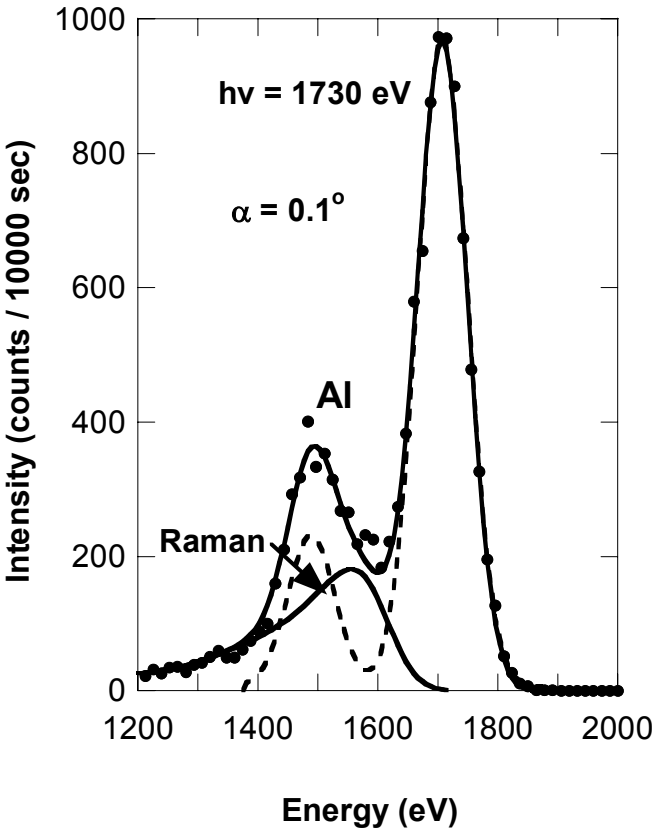
1000
800
600
400
200
0
1200
1400
1600
1800
2000
hv = 1730 eV
α = 0.1°
Al
Raman
Intensity (counts / 10000 sec)
Energy (eV)

Fig. 2

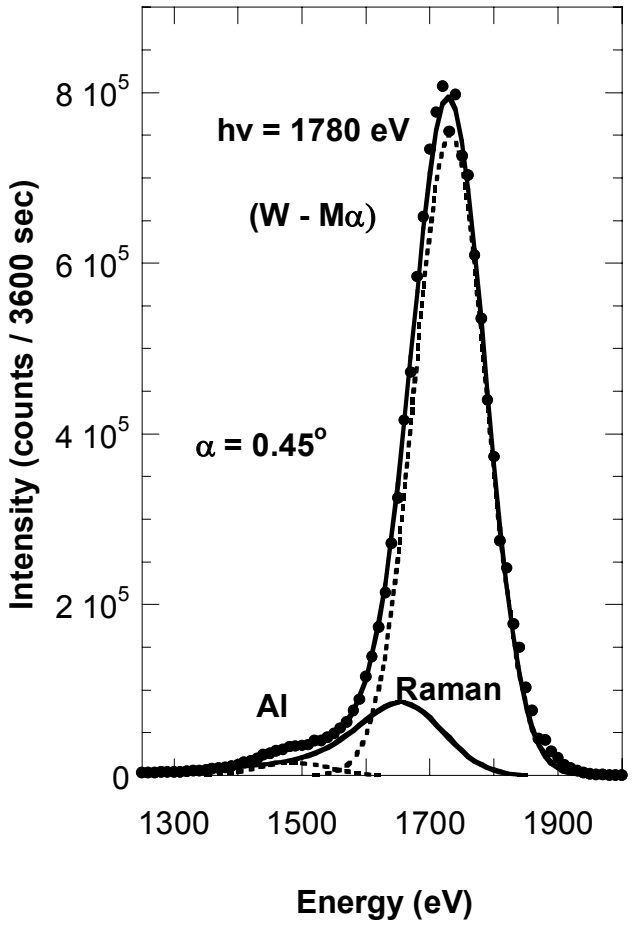
8 10^5
6 10^5
4 10^5
2 10^5
0
Intensity (counts / 3600 sec)
hv = 1780 eV
(W - Mα)
α = 0.45°
Al
Raman
1300
1500
1700
1900
Energy (eV)

Fig. 3

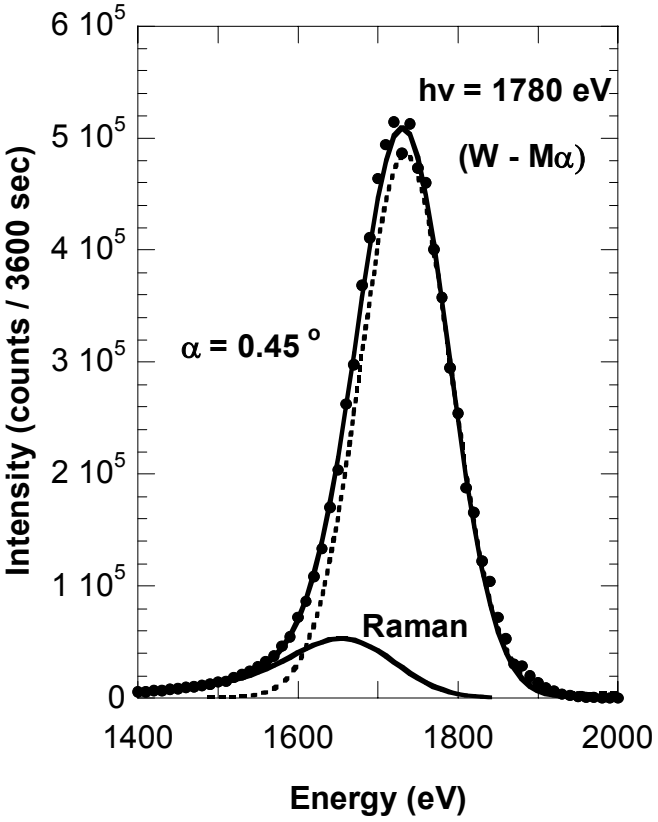
6 10^5
5 10^5
4 10^5
3 10^5
2 10^5
1 10^5
0
Intensity (counts / 3600 sec)
hv = 1780 eV
(W - Mα)
α = 0.45 °
Raman
1400
1600
1800
2000
Energy (eV)

Fig. 4

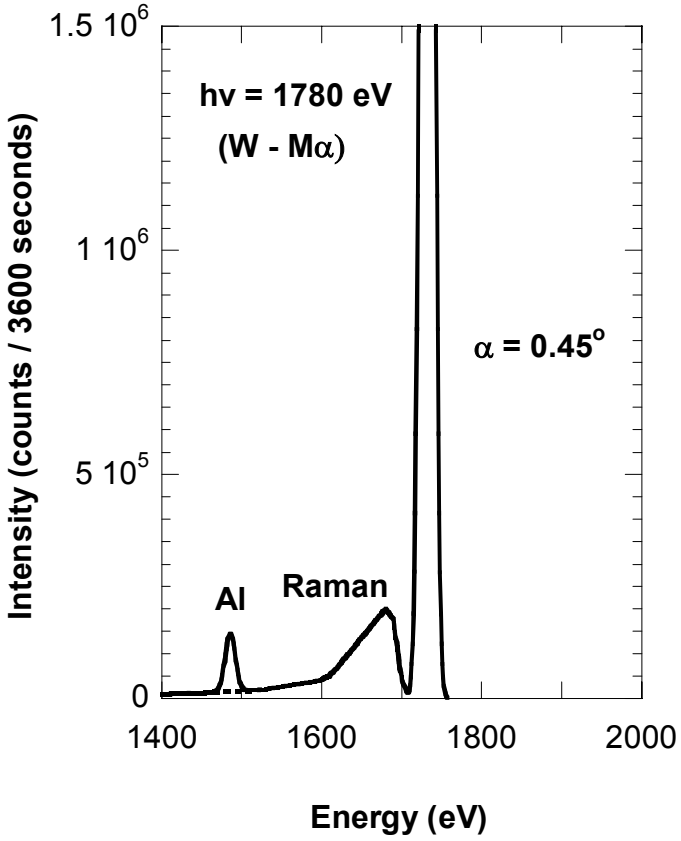
1.5 10^6
1 10^6
5 10^5
0
Intensity (counts / 3600 seconds)
hv = 1780 eV
(W - Mα)
α = 0.45°
Al
Raman
1400
1600
1800
2000
Energy (eV)

Fig. 5

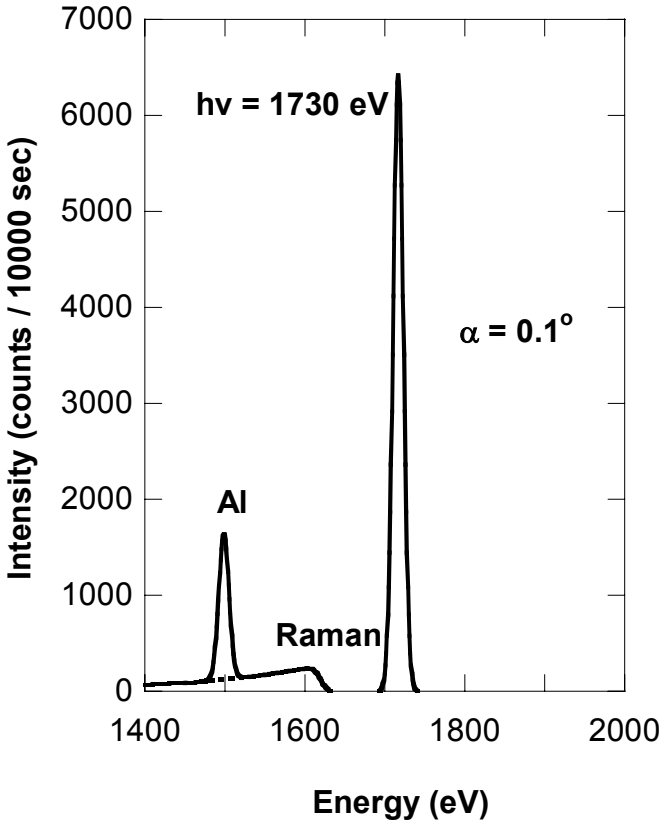
7000
6000
5000
4000
3000
2000
1000
0
Intensity (counts / 10000 sec)
hv = 1730 eV
α = 0.1°
Al
Raman
1400
1600
1800
2000
Energy (eV)

Fig. 6